Supporting Information

A Solution-Processable Wholly-aromatic Bipolar Host Material for Highly Efficient Blue Electroluminescent Devices

Jie Yuan*[ab], He Jiang[b], Qingqing Yang[b], Yuan Xiang[b], Ying Zhang[b], Yizhong Dai[b], Ping Li[b], Chao Zheng[b], Guohua Xie*[c] and Runfeng Chen*[b]

[a]*Engineering Technology Training Center, Nanjing Institute of Industry Technology, 1 Yangshan North Road, Nanjing 210023, China*

[b]*Key Laboratory for Organic Electronics and Information Displays & Jiangsu Key Laboratory for Biosensors, Institute of Advanced Materials (IAM), Jiangsu National Synergetic Innovation Center for Advanced Materials (SICAM), Nanjing University of Posts & Telecommunications, 9 Wenyuan Road, Nanjing 210023, China.*

[c]*Sauvage Center for Molecular Sciences, Hubei Key Lab on Organic and Polymeric Optoelectronic Materials, Department of Chemistry, Wuhan University, Wuhan, 430072, China.*

Content

1. Synthesis and Characterization

Unless otherwise noted, chemicals and solvents purchased from Aldrich or Acros are of analytical grade, and were used without further purification. ^{1}H and ^{13}C-nuclear magnetic resonance (NMR) spectra were recorded on a Bruker Ultra Shield Plus 400 MHz instrument with $CDCl_3$ or dimethyl sulfoxide-D6 (DMSO-D6) as the solvent and tetramethylsilane (TMS) as the internal standard. Matrix-Assisted Laser Desorption/ Ionization Time of Flight Mass Spectrometry (MALDI-TOF-MS) spectrum was measured on a Bruker Autoflex Speed TOF/TOF. Elemental analysis was performed on an Elementar Vario MICRO elemental analyzer.

9H-thioxanthen-9-one 10,10-dioxide (ThX): To a 250 mL round bottom flask charged with a stir bar, hydrogen peroxide (35% aqueous solution, 0.16 g, 4.71 mmol) was added to a stirred solution of thioxanthen-9-one (1.00 g, 4.71 mmol) in acetic acid (20 mL) at 20°C.[1] The resulting mixture was put under reflux for 2 h and was then cooled to 20°C to yield a precipitate, which was filtered and washed with hexane to produce yellow crystals (yield = 83%). ^{1}H NMR (400 MHz, $CDCl_3$, ppm): δ=8.35 (dd, J=7.5 Hz, J=1.5 Hz, 2H), 8.19 (dd, J=7.5 Hz, J=1.5 Hz, 2H), 7.88 (td, J=8 Hz, J=1.5 Hz, 2 H), 7.78 (td, J=8 Hz, J=1.5 Hz, 2H); ^{13}C NMR (400 MHz, $CDCl_3$, ppm): δ=178.6, 141.2, 134.9, 133.5, 130.9, 129.4, 123.8.

9,9-bis(9-phenyl-9H-carbazol-3-yl)-9H-thioxanthene 10,10-dioxide (BPhCz-ThX): Under nitrogen atmosphere, 9-9-phenyl-9H-carbazol (1.00 g, 4.10 mmol) and 9H-thioxanthe-9-one-S,S-dioxide (0.25 g, 1.02 mmol) were placed in an oven-dried round-bottom schlenk flask at room temperature. Under a stream of nitrogen, the starting material was heated to be fully melted at 90°C. Then, Eaton's reagent (0.1 mL) was added drop-wise for over 30 min, and the mixture was stirred under nitrogen for another 12 h.[2] To end the reaction, the mixture was cooled, and the MeOH (10 mL) was added into and stirred for another 2 h. The reaction mixture was diluted with dichloromethane (DCM), washed with brine, and extracted with DCM for three times. The organic layers were collected and dried over $MgSO_4$ and the solvent was removed in vacuum to produce a crude dark-gray powder. The crude product was suspended in acetone and refluxed overnight until a fine white powder was obtained. Further, the product was purified by vacuum sublimation. The final product was a white solid (yield = 76%). ^{1}H NMR (400 MHz, DMSO, ppm): δ= 8.17 (d, J=4 Hz, 1H), 8.15 (s, 1H), 7.87 (s, 1 H), 7.85 (s, 1H), 7.71 (m, 14H), 7.51 (dd, J=12 Hz, 2H), 7.39 (m, 6H), 7.20 (m, 4H), 6.90 (dd, J=8 Hz, 2H); ^{13}C NMR (400 MHz, DMSO-D6, ppm): δ= 146.26,

141.04, 139.41, 137.21, 137.11, 137.07, 133.05, 132.69, 130.67, 129.00, 128.93, 128.22, 127.05, 127.00, 123.83, 122.94, 122.65, 122.14, 120.85, 120.68, 110.24, 109.85, 59.11. MALDI-TOF-MS (CH_2Cl_2) *m/z*: calculated for $C_{49}H_{32}N_2O_2S$: 712.221; Found: 711.879. Elemental Analysis: Anal. calcd. for $C_{49}H_{32}N_2O_2S$: C, 82.56; H, 4.52; N, 3.93; S, 4.50; Found: C, 82.42; H, 4.42; N, 3.93; S, 4.06.

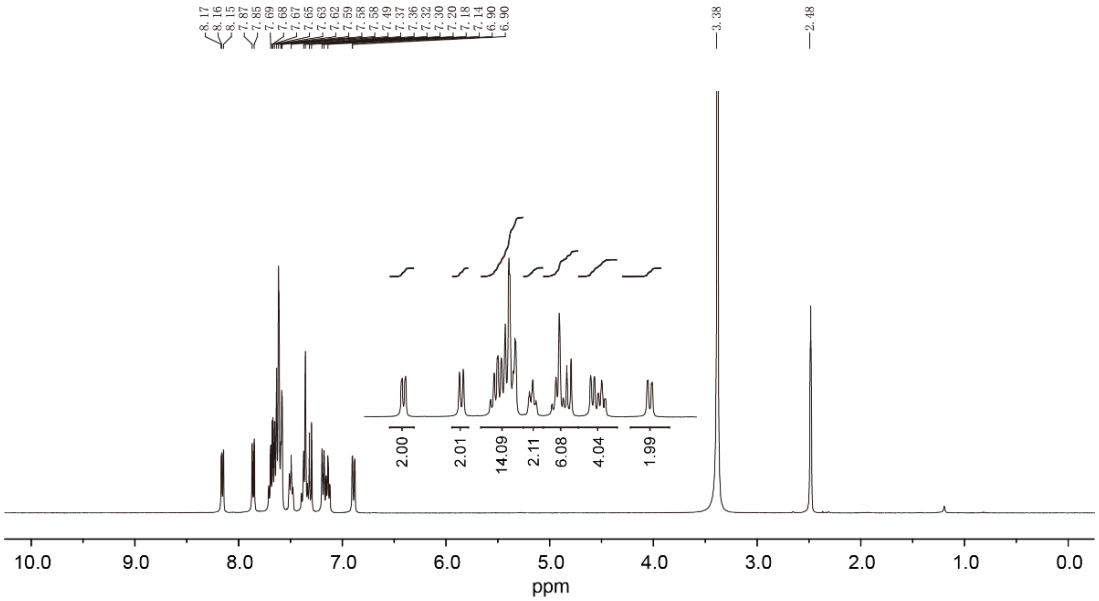

Figure S1. ^{1}H NMR of **BPhCz-ThX** in DMSO-D6**.**

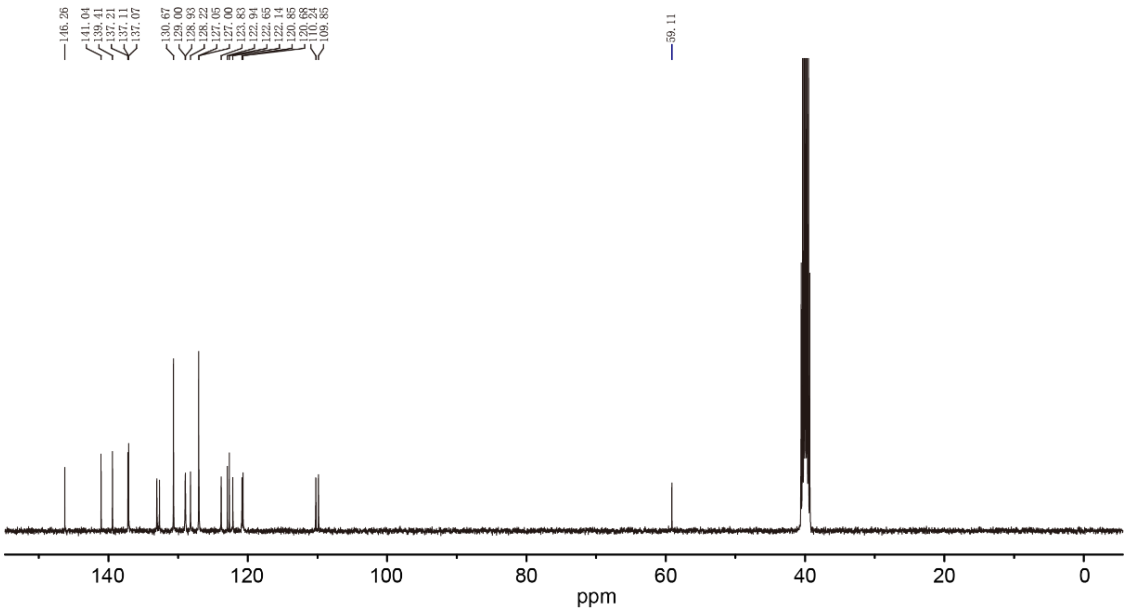

Figure S2. ^{13}C NMR of **BPhCz-ThX** in DMSO-D6**.**

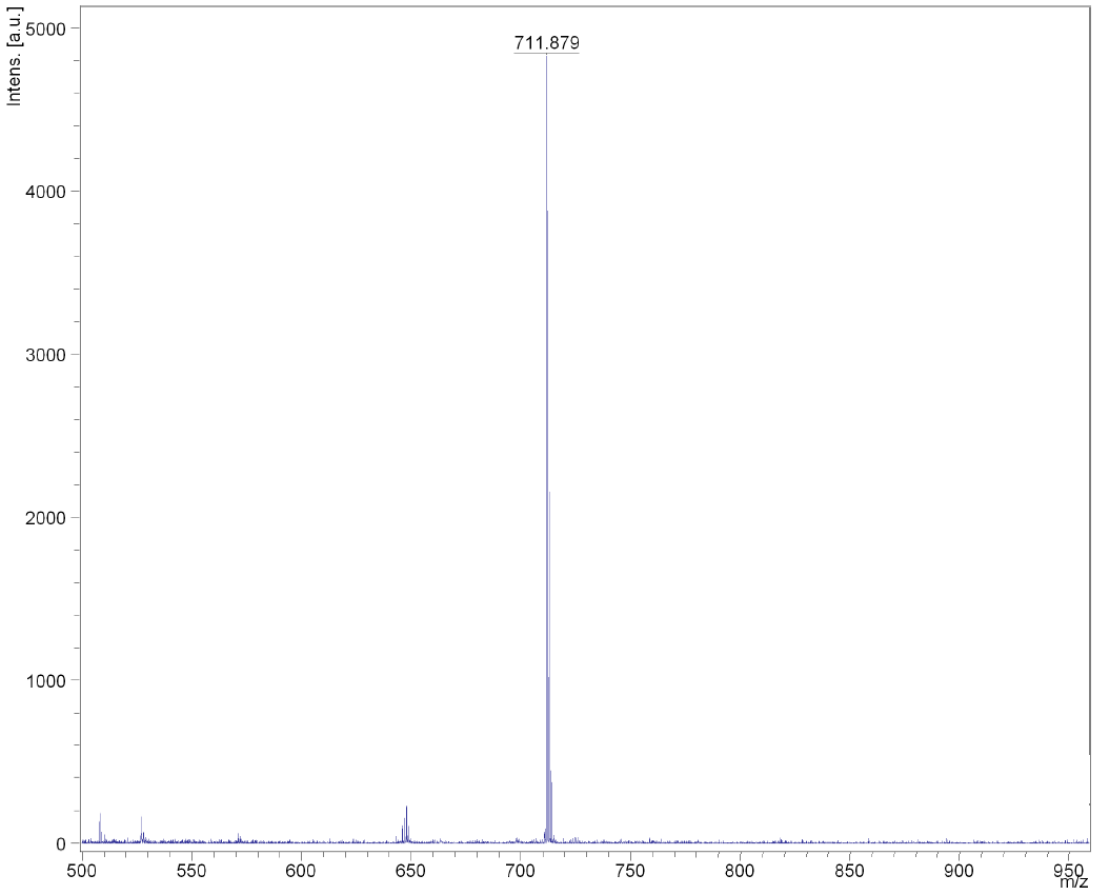

Figure S3. MALDI-TOF-MS spectrum of **BPhCz-ThX.**

2. Thermal Property

Thermogravimetric analysis (TGA) was conducted on a Shimadzu DTG-60H thermogravimetric analysis under a heating rate of 10ºC/min and a nitrogen flow rate of 50 cm^3/min. The differential scanning calorimetry (DSC) analysis was performed on a Shimadzu DSC-60A instrument under a heating rate of 10°C/min and a nitrogen flow rate of 20 cm^3/min. Thermal decomposition temperature (T_d) is defined as the temperature when the sample's weight loss reaches 5%.

3. Optical Properties

Ultraviolet-visible (UV-Vis) spectra were obtained using a SHIMADZU UV-3600 UV-VIS-NIR spectrophotometer. Steady-state and time-resolved photoluminescence were measured on an Edinburgh FLSP920 fluorescence spectrophotometer.

4. Electrochemical property

Cyclic voltammetry (CV) measurement was performed to estimate the highest occupied

molecular orbital (HOMO) and the lowest unoccupied molecular orbital (LUMO) from the onset potential of the electrochemical oxidation and reduction waves, respectively.[3] The CV measurements were carried out on a CHI660E system in a typical there-electrode cell with a working electrode (glass carbon) at room temperature, a reference electrode (Ag/Ag^+), referenced against ferrocene/ferrocenium (FOC), and a counter electrode (Pt wire) in an acetonitrile solution of Bu4NPF6 (0.1 M) at a sweeping rate of 100 mV s^{-1}. The thin solid film of the optoelectronic molecule was deposited on the surface of the glass carbon working electrode for CV measurement. HOMO and LUMO energy levels (E_{HOMO} and E_{LUMO}) were estimated based on the reference energy level of ferrocene (4.8 eV below the vacuum) according to the following Equations:

$$E_{HOMO} = -[E_{onset}^{Ox} - E_{(Fc/Fc^+)} + 4.8]\, eV \qquad \text{(S1)}$$

$$E_{LUMO} = -[E_{onset}^{Red} - E_{(Fc/Fc^+)} + 4.8]\, eV \qquad \text{(S2)}$$

where $E_{(Fc/Fc+)}$ is the onset oxidative voltage of FOC *vs* Ag/Ag^+ and E_{onset}^{Ox} and E_{onset}^{Red} are the onset potentials of the oxidationare and reduction, respectively.

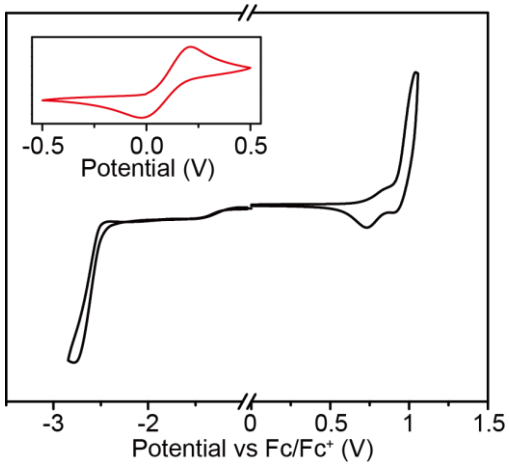

Figure S4. Cyclic voltammogram curve of **BPhCz-ThX** film. The insert graph shows the oxidation wave of ferrocene under the identical electrochemical conditions.

Table S1. Thermal, photophysical, and electrochemical properties of **BPhCz-ThX** [a].

Compound	$T_g/T_m/T_d$ (℃)	${}^s\lambda_{abs}$ (nm)	${}^f\lambda_{abs}$ (nm)	${}^s\lambda_{PL}$ (nm)	${}^f\lambda_{PL}$ (nm)	${}^{opt}E_g$ (eV)	HOMO/LUMO (eV)	E_T (eV)
BPhCz-ThX	138/205/464	298/333/346	302/335/349	355/371	358/372	3.56	-5.53/-2.34	3.05

[a]Absorption (abs) peaks measured in CH_2Cl_2 solution (${}^s\lambda_{abs}$) and thin film (${}^f\lambda_{abs}$) as well as photoluminescent (PL) peaks observed in CH_2Cl_2 solution (${}^s\lambda_{PL}$) and thin film (${}^f\lambda_{PL}$) at the room temperature. Optical energy gap (${}^{opt}E_g$) was obtained from the onset of UV-vis spectrum in solid film. HOMO and LUMO energy level were deduced from Equations S1 and S2. Triplet energy (E_T) was determined by the highest energy vibronic sub-band of the phosphorescence spectrum at 77 K.

5. Theoretical calculations

Density functional theory (DFT) and time-dependent DFT (TD-DFT) calculations were carried out on Gaussian 09 D.01 package.[4] The ground state (S_0) geometry was fully optimized at B3LYP/6-31G(d) level and the optimized stationary point was further characterized by harmonic vibration frequency analysis to ensure that real local minima had been found. The excitation energies in the *n*-th singlet (S_n) and triplet (T_n) states were computed using the TD-DFT method based on the optimized molecular structure at the ground state (S_0). Contour of electrostatic potential (ESP) were obtained also on the ground state geometry to investigate the charge density distribution.[5] The color code of the map was from the deepest red to the deepest blue, when the potential increases in the order of red < orange < yellow < green < blue.

The charge injection, transport and their balance are crucial for optoelectronic devices; therefore, it is important to investigate the ionization potentials (IPs), hole extraction potentials (HEPs), electronic affinities (EAs), electron extraction potentials (EEPs) and reorganization energies (λ) of optoelectronic molecules to evaluate the energy barrier for injection and transport rates of the hole and electron.[6] The charge (hole and electron) mobility of **BPhCz-ThX** was assessed using the incoherent hopping model, which assumes a charge transport process between two adjacent reactions $M^{\pm} + M \rightarrow M + M^{\pm}$, where M is the neutral molecule interacting with neighboring oxidized or reduced $M^{\pm}$. The hopping rates of charge transfer can be described by the Marcus−Hush equation:[7]

$$K_{h/e} = \left(\frac{\pi}{\lambda_{h/e} kT}\right)^{1/2} \frac{V_{h/e}^2}{\hbar} \exp\left(-\frac{\lambda_{h/e}}{4kT}\right) \quad \text{(S3)}$$

where $V_{h/e}$ is the electronic coupling matrix element between neighboring molecules; T is the temperature; k and ħ refer to the Boltzmann and Planck constants, respectively; $\lambda_{h/e}$ is the hole/electron reorganization energy calculated by the following equations:

$$\lambda_h = \lambda_+ + \lambda_1 \quad \text{(S4)}$$

$$\lambda_e = \lambda_- + \lambda_2 \quad \text{(S5)}$$

$$\lambda_+ = E^+(M) - E^+(M^+) \quad \text{(S6)}$$

$$\lambda_1 = E(M^+) - E(M) \quad \text{(S7)}$$

$$\lambda_- = E^-(M) - E^-(M^-) \quad \text{(S8)}$$

$$\lambda_2 = E(M^-) - E(M) \quad \text{(S9)}$$

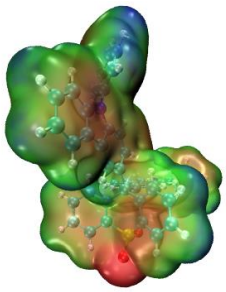

Figure S5. DFT calculated isosurface of electrostatic potential (ESP) of **BPhCz-ThX.**

Table S2. Ionization potential (IP), hole extraction potential (HEP), electronic affinity (EA), electron extraction potential (EEP) and reorganization energies (λ_{hole} and $\lambda_{electron}$) of **BPhCz-ThX** calculated by B3LYP/6-31G (d) (in eV).

Compound	IP	HEP	EA	EEP	λ_{hole}	$\lambda_{electron}$
BPhCz-ThX	6.37	6.21	0.01	0.15	0.15	0.14

6. Morphology property

Atomic force microscopy (AFM) height map measurements with a topographic image area of 5 × 5 μm^2 were carried out on a Bruker Dimension Icon AFM equipped with Scanasyst-Air peak force tapping mode AFM tips from Bruker.

7. Devices fabrication and measurement

Blue organic light emitting diodes (OLEDs) using 9,9-bis(9-phenyl-9H-carbazol-3-yl)-9H-thioxanthene 10,10-dioxide (**BPhCz-ThX)** as host material were fabricated by using Iridium(III) [bis(4,6-difluorophenyl)-pyridinato-N,C2'] picolinate (FIrpic) and 10-(4-((4-(9H-Carbazol-9-yl)phenyl)sulfonyl)phenyl)-9,9-dimethyl-9,10-dihydroacridine (CzAcSF) as the blue phosphorescent and thermal active delay fluorescent (TADF) doped emitters, respectively. Similarly, poly(3,4-ethylenedioxythiophene): poly(styrenesulfonate) (PEDOT: PSS) and 8-Hydroxyquinolinolato-lithium (Liq) are functioned as hole- and electron-injecting layers, respectively. 1,3,5-Tri(m-pyrid-3-yl-phenyl)benzene (TmPyPB) is used as the electron-transporting layer (ETL) while bis[2-(diphenylphosphino)phenyl]ether oxide (DPEPO) acts as exciton-blocking layer. The blue phosphorescence OLED (PhOLED) was fabricated in a device structure of ITO/PEDOT: PSS (40 nm)/host: 15 wt% FIrpic (50 nm)/DPEPO (10 nm)/TmPyPB (50 nm)/Liq (1 nm)/Al (100 nm) and the blue TADF OLED was fabricated with a device structure of ITO/PEDOT:PSS (40 nm)/host: 15 wt% CzAcSF (50 nm)/DPEPO (10 nm)/TmPyPB (50 nm)/Liq (1 nm)/Al (100 nm).[8] Single-carrier transporting devices based on **BPhCz-ThX** were fabricated with configurations of ITO/Liq (1 nm)/TmPyPB (50 nm)/**BPhCz-ThX** (50 nm)/TmPyPB (50 nm)/Liq (1 nm)/Al (100 nm) for electron-only and ITO/PEDOT: PSS (40 nm)/TAPC (20 nm)/ **BPhCz-ThX** (50 nm)/TAPC (20 nm)/PEDOT: PSS (40 nm)/Al (100 nm) for hole-only devices, respectively.[9]

In a general procedure, the patterned ITO glass substrates were ultrasonically cleaned with detergent, alcohol, acetone, and deionized water for 30 min respectively, and then dried at 120°C in a vacuum oven for more than one hour. After ultraviolet (UV)-ozone treating for 15 min, a 40 nm PEDOT: PSS was spin coated on the ITO substrate and dried at 120°C in a vacuum oven for 10 min. Then, the emissive layers (EMLs) containing **BPhCz-ThX** host molecule and FIrpic or CzAcSF as guest molecule were spin-coated on the top of PEDOT: PSS from chlorobenzene (10 mg/ml) and annealed using a hot plate at 50°C for 10 min to remove residual solvents. After that, the samples

were transferred to a thermal evaporator chamber. DPEPO (10 nm), TmPyPB (50 nm), Liq (1 nm), and Al (100 nm) were deposited subsequently by thermal evaporation under a pressure of 5×10^{-4} Pa. The thickness of these vacuum-deposited layers was monitored using a spectroscopic ellipsometry (α-SE, J.A. Wollam Co. Inc.). The devices were measured without encapsulation immediately after fabrication at room temperature under ambient atmosphere conditions. The luminance-current-voltage (L-J-V) characteristics of the devices were recorded by a combination of a Keithley source-meter (model 2602) and a calibrated luminance meter. Electroluminescence (EL) spectra were obtained using a spectra-scan PR735 spectrophotometer. The external quantum efficiency (EQE) was achieved according to Equation S3.[10]

$$EQE = \frac{\pi e \eta_{cd/A} \int \lambda p(\lambda) d\lambda}{hcK_m \int p(\lambda)\Phi(\lambda) d\lambda} \qquad \text{(S10)}$$

where $\eta_{cd/A}$ is the current efficiency (cd/A); h is the Planck constant; c is the speed of light in vacuum; λ is the wavelength (nm); e is the electron charge; $p(\lambda)$ is relative electroluminescent intensity at each wavelength; $\Phi(\lambda)$ is the Commision International de l'Eclairage chromaticity (CIE) standard photopic luminous efficiency function; and K_m is a constant of 683 lm/W.

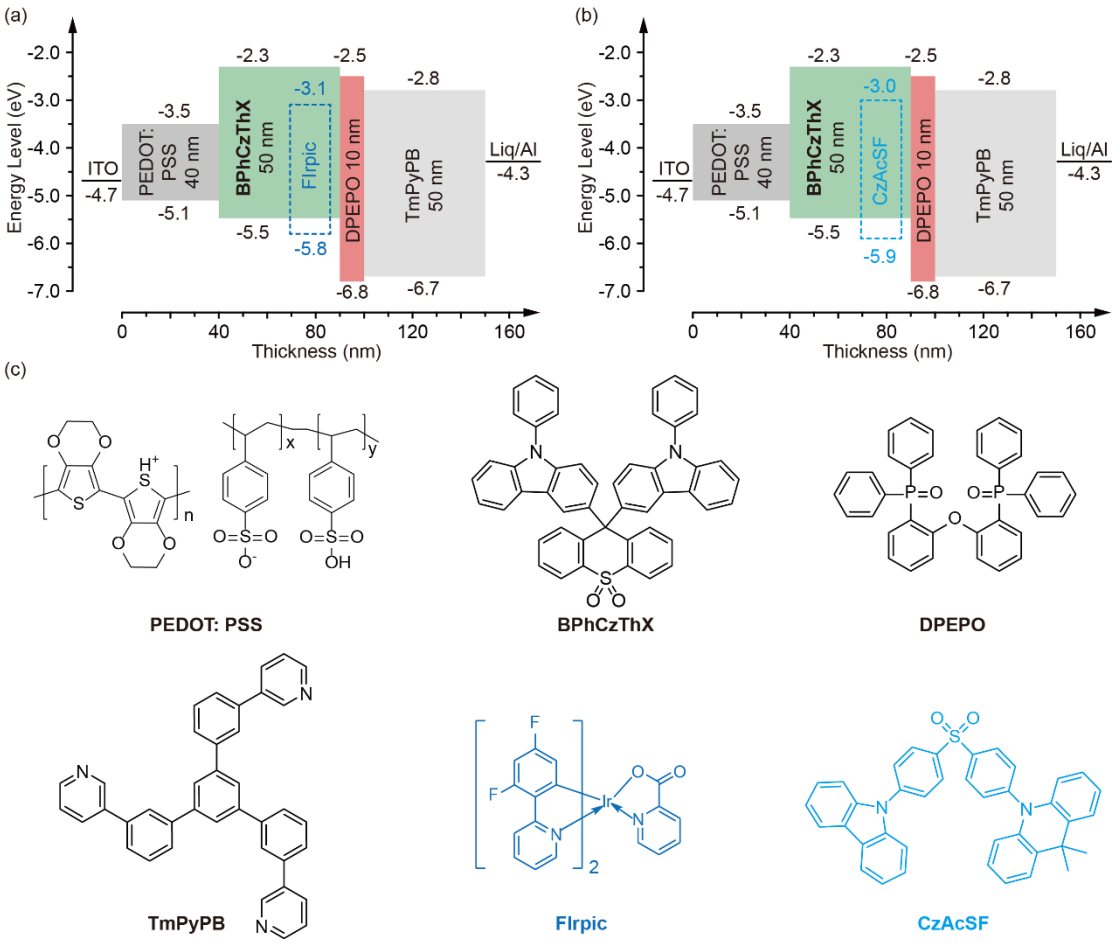

Figure S6. The device configuration and corresponding thickness of each layer and energy level diagram of (a) Device A and (b) Device B, and (c) molecular structures of the materials used in the **BPhCz-ThX**-host spin-coated blue OLEDs.

References

1. I. Lee and J. Y. Lee, *Org. Electron.*, 2016, **29**, 160-164.
2. P.-I. Shih, C.-L. Chiang, A. K. Dixit, C.-K. Chen, M.-C. Yuan, R.-Y. Lee, C.-T. Chen, E. W.-G. Diau and C.-F. Shu, *Org. Lett.*, 2006, **8**, 2799-2802.
3. H. Li, R. Bi, T. Chen, K. Yuan, R. Chen, Y. Tao, H. Zhang, C. Zheng and W. Huang, *ACS Appl. Mater. Inter.*, 2016, **8**, 7274-7282.
4. J. Yin, S.-L. Zhang, R.-F. Chen, Q.-D. Ling and W. Huang, *Phys. Chem. Chem. Phys.*, 2010, **12**, 15448-15458.
5. P. K. Weiner, R. Langridge, J. M. Blaney, R. Schaefer and P. A. Kollman, *P. Natl. Acad. Sci.*, 1982, **79**, 3754-3758.
6. M.-K. Yan, Y. Tao, R.-F. Chen, C. Zheng, Z.-F. An and W. Huang, *RSC Adv.*, 2012, **2**, 7860-7867.
7. Y. Zeng, R. B. Smith, P. Bai and M. Z. Bazant, *J. Electroanal. Chem.*, 2014, **735**, 77-83.
8. X. Zheng, R. Huang, C. Zhong, G. Xie, W. Ning, M. Huang, F. Ni, F. B. Dias and C. Yang, *Adv. Sci.*, 2020, **7**, 1902087-1902093.
9. C. Han, Z. Zhang, H. Xu, S. Yue, J. Li, P. Yan, Z. Deng, Y. Zhao, P. Yan and S. Liu, *J. Am. Chem. Soc.*, 2012, **134**, 19179-19188.
10. Y. Tao, J. Xiao, C. Zheng, Z. Zhang, M. Yan, R. Chen, X. Zhou, H. Li, Z. An, Z. Wang, H. Xu and W. Huang, *Angew. Chem. Int. Edit.*, 2013, **52**, 10491-10495.